Supplement of Atmos. Meas. Tech., 18, 4087–4102, 2025
https://doi.org/10.5194/amt-18-4087-2025-supplement

Atmospheric Measurement Techniques
Open Access

Supplement of

Vertical distribution of halogenated trace gases in the summer Arctic stratosphere based on two independent air sampling methods

Johannes C. Laube et al.

Correspondence to: Johannes C. Laube (j.laube@fz-juelich.de)

Summary of the comparison of CRYO measurements

As mentioned in Section 2.4, the CRYO samples were analysed with three different analytical systems, but brought onto consistent calibration scales (Table S1) through concurrent measurements of a clean-air standard in both labs. Out of the 288 cases (13 samples by 24 gases, with 24 cases of mole fractions below detection limit), agreement within two standard deviations were found in all but 13 cases; nine of which still agree within three standard deviations (Table S2). For two of the remaining cases, the sample with the lowest detected mole fraction for CFC-11 and H-1211 did not agree between measurement systems, which points towards a nonlinear response behaviour of one or both systems at very low mole fractions for those two species. Since analytical non-linearities at ultra-low mole fractions are very work-intensive to adequately quantify, and these cases have no significant impact on the main conclusions of this manuscript, these were simply merged and the uncertainty ranges increased accordingly. The remaining two cases concern $CHCl_3$, for which consistently lower mole fractions were found during the later analysis at FZJ. This is most likely caused by a lack of long-term stability of this (and other shorter-lived) compounds in the CRYO canisters, which has been observed before (Laube et al., 2008). As agreement within three standard deviations was still observed for nine samples, we nevertheless merged the mole fractions from the two lab analyses. However, we do not report CRYO-based mole fractions of other short-lived species here as their stability could not be constrained due to the remaining air being used for isotope measurements (not part of this study).

Table S1. Details of the trace gases quantified from both samplers via the different measurement systems, including average precisions and calibration scales.

Species (formula)	NOAA GML Mixing ratio @ Barrow [ppt]*	Sampler	Lab	Measured @ m/z (rounded to full digits)	Average precision (MAC_small, MAC_large, CRYO_FZJ, CRYO_GUF)	Calibration scale	Comment
CFC-11 (CCl3F)	220.75 ± 0.45	MAC+CRYO	FZJ, GUF	103 (FZJ), 101 (GUF)	1.4, 0.6, 0.5, 0.5	NOAA 2016 GC-ECD	-
CFC-112 (CCl2FCCl2F)	N/A	MAC+CRYO	FZJ, GUF	103	3.0, 2.2, 1.0, 4.0	UEA 2012	-
CFC-113 (CCl2FCClF2)	69.22 ± 0.22	MAC+CRYO	FZJ, GUF	103 (FZJ), 151 (GUF)	1.1, 0.5, 0.4, 0.7	NOAA 2002 GC-ECD	-
CFC-113a (CCl3CF3)	N/A	MAC+CRYO	FZJ	121	14.6, 4.3, 1.6, N/A	UEA 2012	-
CFC-115 (C2ClF5)	N/A	MAC+CRYO	FZJ, GUF	85	0.6, 0.6, 0.4, 0.8	SIO-05	-
CFC-12 (CCl2F2)	492.25 ± 0.69	MAC+CRYO	FZJ, GUF	101 (FZJ), 85 (GUF)	1.1, 0.7, 0.6, 0.5	NOAA 2008 GC-ECD	(5)
CFC-13 (CClF3)	N/A	MAC+CRYO	FZJ	87	N/A, 2.2, 1.5, N/A	METAS-2017	-
CCl4	75.92 ± 0.25	MAC+CRYO	FZJ, GUF	121 (FZJ), 117 (GUF)	7.8, 1.8, 1.0, 0.7	NOAA 2008 GC-MS	(6)
CH3CCl3	1.36 ± 0.08	MAC+CRYO	FZJ, GUF	97	6.8, 3.5, 3.5, 2.4	NOAA 2003 GC-ECD	-
H-1202 (CBr2F2)	N/A	CRYO	FZJ	129	N/A, N/A, 8.4, N/A	UEA 1998	-
H-1211 (CBrClF2)	3.04 ± 0.01	MAC+CRYO	FZJ, GUF	129 (FZJ), 85 (GUF)	3.0, 1.0, 0.5, 1.4	NOAA 2006 GC-ECD	-
H-1301 (CBrF3)	3.378 ± 0.013 (1)	MAC+CRYO	FZJ, GUF	148 (FZJ), 69 (GUF)	1.8, 1.0, 0.7, 1.6	NOAA 2006 GC-ECD	-
H-2402 (CBrF2CBrF2)	N/A	MAC+CRYO	FZJ, GUF	129 (FZJ), 179 (GUF)	12.3, 3.1, 1.9, 2.7	UEA 1998	-
HCFC-133a (CH2ClCF3)	N/A	MAC+CRYO	FZJ, GUF	118	8.9, 1.8, 0.6, 4.3	UEA 2012	-
HCFC-141b (CH3CCl2F)	N/A	MAC+CRYO	FZJ, GUF	103 (FZJ), 81 (GUF)	1.7, 1.4, 1.3, 1.1	NOAA 1994 GC-MS	-
HCFC-142b (CH3CClF2)	N/A	MAC+CRYO	FZJ, GUF	65	1.2, 0.6, 0.5, 0.5	NOAA 1994 GC-MS	-
HCFC-22 (CHClF2)	N/A	MAC+CRYO	FZJ, GUF	67 (FZJ), 51 (GUF)	0.5, 0.8, 0.6, 0.7	NOAA 2006 GC-MS	-
HFC-125 (C2HF5)	38.028 ± 0.110 (1)	MAC+CRYO	FZJ, GUF	101 (FZJ), 51 (GUF)	0.9, 0.7, 0.8, 0.8	UB-98	-
HFC-134a (CH2FCF3)	126.88 ± 0.25 (1)	MAC+CRYO	FZJ, GUF	102 (FZJ), 101 (GUF)	2.3, 1.3, 1.4, 0.7	NOAA 1995 GC-MS	(5)
HFC-143a (CH3CF3)	28.744 ± 0.128 (2)	MAC+CRYO	FZJ, GUF	65 (FZJ), 33 (GUF)	1.9, 0.9, 0.6, 0.9	SIO-07	-
HFC-152a (CH3CHF2)	N/A	CRYO	GUF	51	N/A, N/A, N/A, 0.9	SIO-05	-
HFC-227ea (CF3CHFCF3)	N/A	MAC+CRYO	FZJ, GUF	151 (FZJ), 69 (GUF)	2.4, 0.6, 0.7, 1.8	UEA 2010	(5)
HFC-23 (CHF3)	N/A	MAC+CRYO	FZJ, GUF	51 (FZJ), 69 (GUF)	0.4, 0.8, 0.6, 2.6	UEA 1998	(5)
HFC-236fa (CF3CH2CF3)	N/A	CRYO	GUF	133	N/A, N/A, N/A, 7.5	SIO-14	-
HFC-245fa (CHF2CH2CF3)	N/A	CRYO	GUF	115	N/A, N/A, N/A, 3.2	SIO-14	-
HFC-32 (CH2F2)	28.700 ± 0.125 (1)	MAC+CRYO	FZJ, GUF	51	2.7, 0.9, 0.6, 1.6	SIO-2007	(5)
PFC-116 (C2F6)	N/A	MAC+CRYO	FZJ	119	1.0, 1.0, 1.2, N/A	UEA 1994	-
PFC-218 (C3F8)	N/A	MAC+CRYO	FZJ	169 (FZJ), 69 (GUF)	19.3, 3.1, 0.7, N/A	UEA 2010	(7)
PFC-318 (cC4F8)	N/A	MAC+CRYO	FZJ, GUF	131	7.8, 0.9, 0.7, 1.1	UEA 2010	(5)
n-C4F10	N/A	CRYO	FZJ	119	N/A, N/A, 4.2, N/A	UEA 2010	-
SF5CF3	N/A	MAC+CRYO	FZJ	89	N/A, 6.2, 5.0, N/A	UEA 1999	(7)
SF6	10.888 ± 0.009	MAC+CRYO	FZJ, GUF(4)	127 (FZJ), N/A (GUF)	0.3, 0.8, 0.5, 0.6	NOAA 2014 GC-ECD	-
SO2F2	2.569 ± 0.077	CRYO	GUF	83	N/A, N/A, N/A, 1.6	SIO-07	-
CH3Cl	N/A	CRYO	GUF	50	N/A, N/A, N/A, 1.1	SIO-05	(6)
CH3Br	6.31-6.59 ± 0.29 (3)	MAC+CRYO	FZJ, GUF	94	N/A, N/A, N/A, 0.5	SIO-05	(8)
CH2Cl2	63.3-70.2 ± 0.43 (3)	MAC+CRYO	FZJ, GUF	84	N/A, N/A, N/A, 1.2	NOAA 2003 GC-MS	(6)
CHCl3	N/A	MAC+CRYO	FZJ, GUF	121 (FZJ), 83 (GUF)	1.2, 0.3, 2.0, 0.7	NOAA 1992 GC-MS	(6)

*from https://gml.noaa.gov/dv/data/ as accessed on 8th August 2024; August 2021 monthly means unless otherwise specified

(1) from sample collected on 13th August 2021

(2) from sample collected on 20th August 2021

(3) from three samples collected between 3rd and 20th August 2021

(4) measured with GC-ECD (see Schuck et al., 2024)

(5) contamination in 1-3 of the MAC subsamplers (but in none of the 6 400-ml-SilcoCans)

(6) Previously reported long-term concentration changes in CRYO (see Laube et al., 2008) - not constrained here

(7) bad precisions in MAC due to low signal

(8) problems with high blanks @ FZJ measurement system

Table S2. Comparability of results from the CRYO sampler between different measurement systems. Listed in each cell are agreement within one, two, and three standard deviations, with “n” referring to “no” and “y” to “yes”. Colouring also refers to agreement within one (white), two (yellow), three (orange), or more (red) standard deviations. Blue fields indicate that the species was not detected by one or both measurement systems. The five columns on the righthand side represent the sum of data agreement cases for each species and have the same colour coding as the main part of the table.

Species (formula)	CRYO_Sample_ID (FZJ/GUF agreement within 1,2, and 3 standard deviations)																		
	1-cat	3	4-cat	5	6	8	9	10-cat	11	12	13-cat	14	15						
CFC-11 (CCl3F)	n,y,y	n,y,y	y,y,y	n,n,y	n,y,y	n,n,n	y,y,y	n,y,y	n,y,y	n,y,y	n,y,y	n,y,y	n,y,y		2	9	1	1	0
CFC-112 (CCl2FCCl2F)	y,y,y	y,y,y	y,y,y	n.d. (1)	y,y,y	n.d. (1)	n.d. (1)	y,y,y	y,y,y	n.d. (1)	y,y,y	y,y,y	y,y,y		9	0	0	0	4
CFC-113 (CCl2FCClF2)	y,y,y	y,y,y	y,y,y	y,y,y	n,y,y	n,y,y	n,y,y	y,y,y	n,y,y	n,y,y	n,y,y	n,y,y	n,y,y		5	8	0	0	0
CFC-115 (C2ClF5)	n,y,y	n,y,y	y,y,y	n,y,y	y,y,y	n,y,y	n,y,y	y,y,y	n,y,y	n,y,y	n,y,y	y,y,y	y,y,y		5	8	0	0	0
CFC-12 (CCl2F2)	y,y,y	y,y,y	y,y,y	y,y,y	y,y,y	y,y,y	y,y,y	n,y,y	y,y,y	y,y,y	y,y,y	y,y,y	y,y,y		12	1	0	0	0
CCl4	y,y,y	y,y,y	y,y,y	n.d. (1)	y,y,y	n.d. (1)	n,y,y	y,y,y	y,y,y	n.d. (1)	y,y,y	y,y,y	y,y,y		9	1	0	0	3
CH3CCl3	y,y,y	n,y,y	y,y,y	n.d. (1)	y,y,y	n.d. (1)	n.d. (1)	y,y,y	n,y,y	n.d. (1)	y,y,y	n.d. (1)	n,y,y		5	3	0	0	5
H-1211 (CBrClF2)	n,y,y	n,y,y	n,y,y	n.d. (1)	y,y,y	n.d. (1)	n,n,n	y,y,y	y,y,y	n.d. (1)	y,y,y	n,y,y	y,y,y		5	4	0	1	3
H-1301 (CBrF3)	y,y,y	y,y,y	n,y,y	n.d. (1)	y,y,y	n,y,y	n,y,y	y,y,y	y,y,y	y,y,y	n,y,y	y,y,y	y,y,y		8	4	0	0	1
H-2402 (CBrF2CBrF2)	y,y,y	y,y,y	n,n,y	n.d. (1)	n,y,y	n.d. (1)	n.d. (1)	y,y,y	y,y,y	n.d. (1)	y,y,y	y,y,y	y,y,y		7	1	1	0	4
HCFC-133a (CH2ClCF3)	n,y,y	y,y,y	n,y,y	n.d. (1)	y,y,y	y,y,y	y,y,y	y,y,y	y,y,y	y,y,y	n,y,y	n,y,y	y,y,y		8	4	0	0	1
HCFC-141b (CH3CCl2F)	n,y,y	n,y,y	y,y,y	n,n,y	n,y,y	n,y,y	y,y,y	n,y,y	n,y,y	n,y,y	n,y,y	n,y,y	y,y,y		3	9	1	0	0
HCFC-142b (CH3CClF2)	y,y,y	y,y,y	y,y,y	y,y,y	y,y,y	y,y,y	y,y,y	y,y,y	y,y,y	y,y,y	y,y,y	y,y,y	y,y,y		13	0	0	0	0
HCFC-22 (CHClF2)	n,y,y	n,y,y	n,y,y	n,y,y	n,y,y	y,y,y	y,y,y	n,y,y	y,y,y	y,y,y	n,y,y	n,y,y	n,y,y		4	9	0	0	0
HFC-125 (C2HF5)	n,y,y	y,y,y	y,y,y	n,y,y	y,y,y	n,y,y	n,y,y	n,y,y	n,y,y	n,y,y	y,y,y	y,y,y	y,y,y		6	7	0	0	0
HFC-134a (CH2FCF3)	n,y,y	n,y,y	y,y,y	n,y,y	n,y,y	n,y,y	y,y,y	n,y,y	n,y,y	n,y,y	n,y,y	y,y,y	n,y,y		3	10	0	0	0
HFC-143a (CH3CF3)	n,y,y	y,y,y	y,y,y	y,y,y	n,y,y	n,y,y	y,y,y	n,y,y	y,y,y	n,y,y	y,y,y	n,y,y	y,y,y		7	6	0	0	0
HFC-227ea (CF3CHFCF3)	n,y,y	n,y,y	n,y,y	n,y,y	n,y,y	n,y,y	n,y,y	n,y,y	n,y,y	n,y,y	n,y,y	n,y,y	n,y,y		0	13	0	0	0
HFC-23 (CHF3)	n,y,y	n.d. (1)	n,y,y	n,y,y	n,n,y	n,y,y	n,y,y	y,y,y	n,y,y	y,y,y	y,y,y	y,y,y	n,y,y		4	7	1	0	1
HFC-32 (CH2F2)	y,y,y	n,y,y	y,y,y	n,y,y	y,y,y	n,y,y	n,n,y	y,y,y	n,y,y	y,y,y	y,y,y	n,y,y	y,y,y		7	5	1	0	0
PFC-318 (cC4F8)	y,y,y	y,y,y	y,y,y	y,y,y	y,y,y	y,y,y	y,y,y	y,y,y	y,y,y	y,y,y	y,y,y	y,y,y	y,y,y		13	0	0	0	0
SF6	n,y,y	n,y,y	n,y,y	n,y,y	n,y,y	n,y,y	n,y,y	y,y,y	n,y,y	y,y,y	n,y,y	n,y,y	n,y,y		2	11	0	0	0
CH2Cl2	y,y,y	n,y,y	n,y,y	n,y,y	y,y,y	n,y,y	n,y,y	y,y,y	y,y,y	n,y,y	y,y,y	n,y,y	y,y,y		5	8	0	0	0
CHCl3	n,n,y	y,y,y	n,n,y	n,n,n	n,n,y	n.d. (1)	n,n,n	n,y,y	n,n,y	n.d. (1)	y,y,y	n,y,y	n,y,y		2	3	4	2	2

(1) not detected with one or both systems

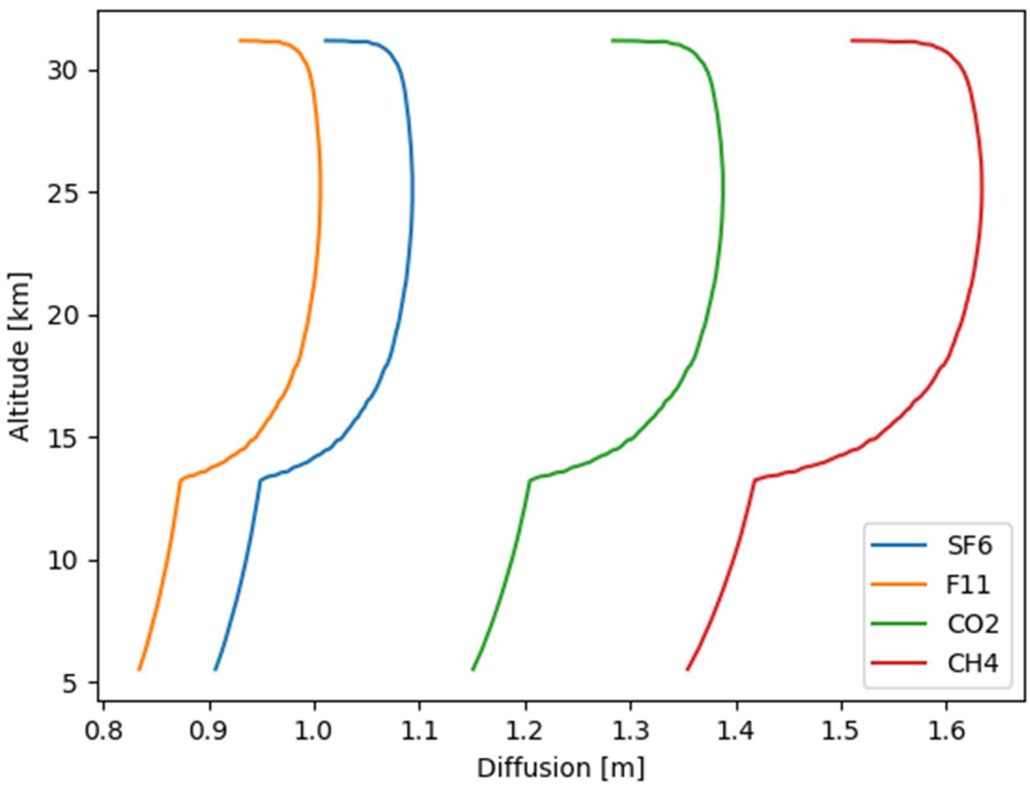

Figure S1. Root mean square molecular diffusion of SF_6, CFC-11, CO_2, and CH_4 inside the MAC tubing as accumulated during flight as well as before and during subsampling. This was calculated as in Tans, 2022: $X_{rms} = \sqrt{2Dt}$ (t: time of air inside MAC) with diffusivity D from Eq. 2 in Kouznetsov et al., 2020: $D = D_0 \frac{p_0}{p} \left(\frac{T}{T_0}\right)^{3/2}$, and molecular diffusivities D_0 from Martinerie et al., 2009. The shape of the curves is due to the competing effects of longer storage times with increasing altitude (air sampled first during the slow balloon descent) and different compression effects (higher near the top due to low ambient pressures). The kink near 12 km is due to the separation of the gondola and the balloon leading to much faster descent speeds below (see Figure 3).

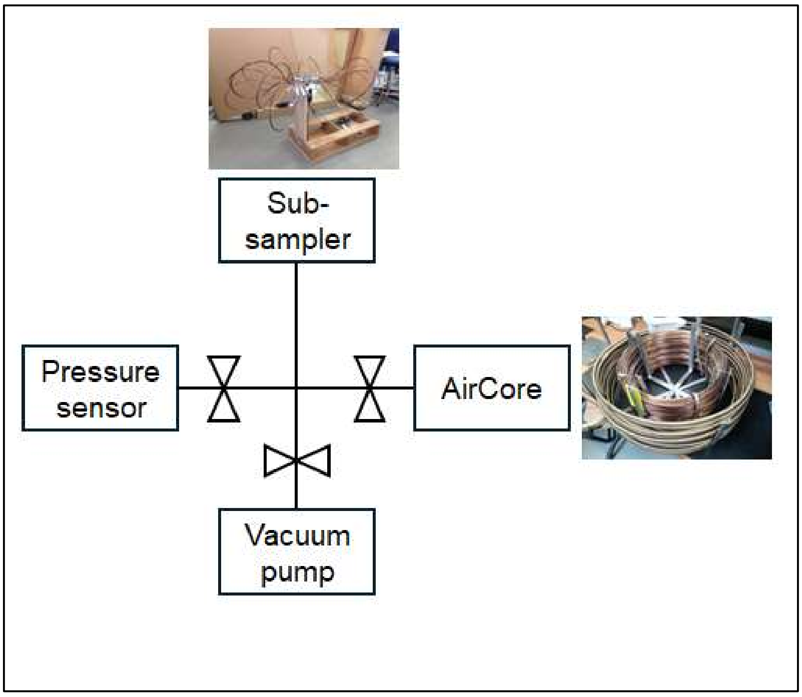

Figure S2. Schematic of the setup for the subsampling of the MAC.

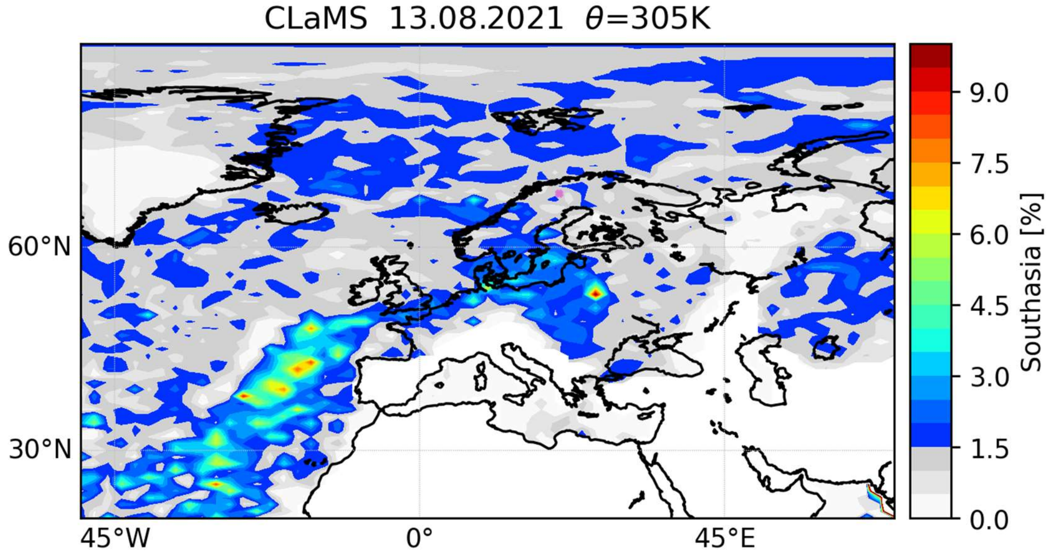

Figure S3. Fraction of an artificial surface origin tracer over northern Europe on 13[th] August 2021 at a potential temperature of 305 K. The tracer was released globally within the Chemical Lagrangian Model of the Stratosphere (CLaMS) and associates the air with the South Asian source region. See Graßl et al. (2024) for further details. The balloon launch location is also marked (pink cross).

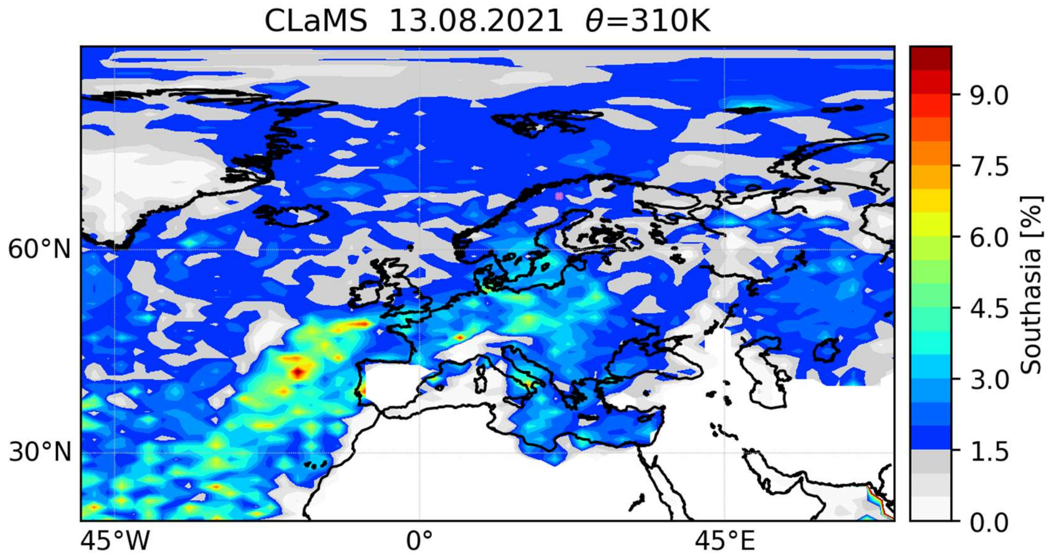

Figure S4. The same as in Figure S3 but at 310 K.

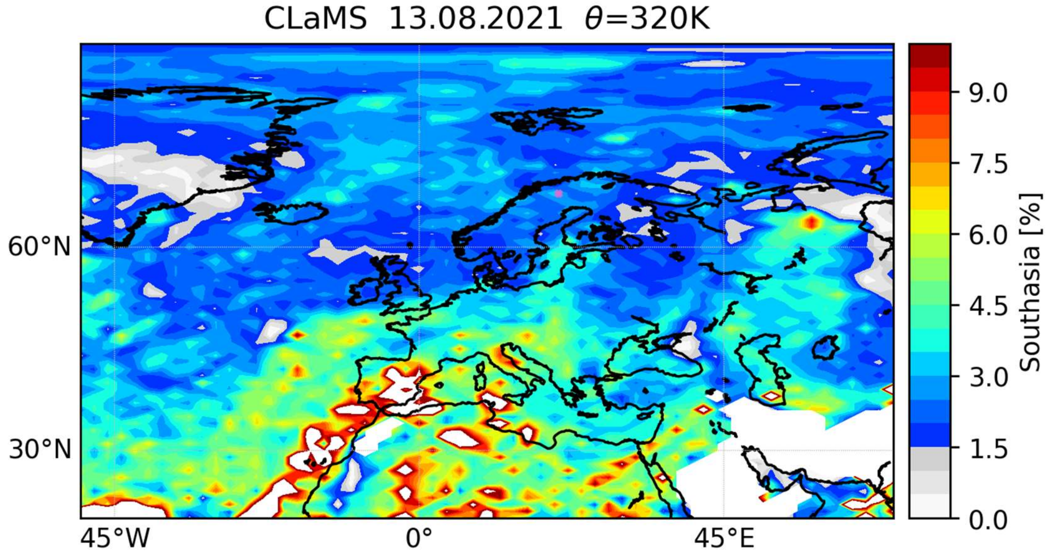

Figure S5. The same as in Figure S3 but at 320 K.